



## **A sustainable functionalization strategy to improving the material properties of bitumen by incorporating graphene**

Downloaded from: <https://research.chalmers.se>, 2025-12-05 01:47 UTC

Citation for the original published paper (version of record):

Jansson, H., Tam, E., Swenson, J. (2024). A sustainable functionalization strategy to improving the material properties of bitumen by incorporating graphene. Next Materials, 4. <http://dx.doi.org/10.1016/j.nxmte.2024.100205>

N.B. When citing this work, cite the original published paper.



## Research article

# A sustainable functionalization strategy to improving the material properties of bitumen by incorporating graphene

Helen Jansson<sup>a,\*</sup>, Pui Lam Tam<sup>b</sup>, Jan Swenson<sup>c</sup>

<sup>a</sup> Department of Architecture and Civil engineering, Division of Building Technology, Chalmers University of Technology, Göteborg SE-412 96, Sweden

<sup>b</sup> Department of Industrial and Materials Science, Division of Materials and Manufacture, Chalmers University of Technology, Göteborg SE-412 96, Sweden

<sup>c</sup> Department of Physics, Division of Nano & Biophysics, Chalmers University of Technology, Göteborg SE-412 96, Sweden

## ARTICLE INFO

## Keywords:

Graphene modified bitumen  
Non-covalent functionalization  
Colloidal stability  
Asphaltenes  
Graphene  
Molecular wedging method  
X-ray photoelectron spectroscopy  
Microscopy

## ABSTRACT

Bitumen is a colloidal system with excellent binder properties, but with poor thermo-mechanical properties. This leads to a poor service life, and as a petroleum derivative this implies a negative environmental impact. To enhance its properties, attempts have been made to modify bitumen with highly thermally conductive nanoparticles, like graphene derivatives. However, the incorporation of graphene derivatives is a challenge due to detrimental interactions between graphene derivatives and asphaltene aggregates, which reduce the colloidal stability. With this study, we show how to not only maintain but also enhance the colloidal stability of bitumen by functionalizing graphene with suitable molecules. By the molecular wedging method, a new and sustainable strategy is developed to overcome any detrimental effects. Thereby, we provide the first successful strategy – a roadmap – to incorporate graphene into bitumen without losing its colloidal stability or negatively affecting the desired properties of graphene.

## 1. Introduction

Despite its extensive use, bitumen has many drawbacks, such as low thermal conductivity, poor energy absorption, high potential for aging, increased oxidation susceptibility, and significantly prone to rutting and fatigue. This leads to a poor service life, and as a petroleum derivative this implies a negative environmental impact [1–3]. Nanoparticles are seen as fillers that can be used to improve its properties. Graphene or graphene derivatives, a family of carbon-based nanoparticles are the most sought-after among the array of nanoparticles due to the excellent thermal, mechanical, and gas barrier properties. However, directly incorporating graphene derivatives into bitumen is a significant scientific and industrial challenge due to rapid graphene-asphaltene aggregation, leading to reduced colloidal stability and phase separation followed by precipitation, see e.g., our previous work [4].

Bitumen is chemically made-up of linear, branched, and cyclic alkanes, as well as monoaromatics and polyaromatic analogies [1,2,5]. It also contains significant amounts of heteroatoms such as oxygen, sulfur, and nitrogen, together with trace amounts of metals in the resin and asphaltene fractions [2]. With such a sizeable elemental composition, the hydrocarbons form constitutional and stereoisomers, leading to nearly 10 s of thousands of structural possibilities, which makes it

extremely complicated to categorize the molecular composition [6]. Therefore, petroleum derivatives are categorized into the various fractions saturates, aromatics, resins, and asphaltenes, also known as SARA fractions [7]. SARA fractions are based on a combined categorization of molecular solubility and molecular polarity/polarizability [2,6–8]. Through the categorization based on solubility, the fractions are divided into the alkane soluble fraction (maltene) and the alkane insoluble fraction (asphaltene). Maltene is, in turn, further divided into a) linear and cyclic alkanes (saturates), b) aromatic hydrocarbons without heteroatoms/polarizable aromatic molecules (aromatics), and c) small aromatic hydrocarbons with heteroatoms/ polar aromatic molecules (resins) [2,6–8].

Asphaltenes are a class of complex heteroatomic polyaromatic hydrocarbons [3,9–11]. They are highly polar and have a single polycyclic aromatic structure with an average size of 7 rings, where about 50% of the asphaltene structure is aromatic while the remaining of the structures are alicyclic and open-chain aliphatic, with alkanes existing in the form of end-functionalized structures [3,9–11]. Saturates are colorless or lightly colored liquids consisting of alkane hydrocarbons in the paraffinic-naphthenic form, which includes linear, branched, and cyclic saturated hydrocarbons [2,3,6–8]. Aromatics, also called naphthene aromatics, is the polarizable fraction, i.e., the SARA fraction with a

\* Corresponding author.

E-mail address: [helen.jansson@chalmers.se](mailto:helen.jansson@chalmers.se) (H. Jansson).

<https://doi.org/10.1016/j.nxmte.2024.100205>

Received 11 December 2023; Received in revised form 4 March 2024; Accepted 10 April 2024

Available online 22 April 2024

2949-8228/© 2024 The Authors. Published by Elsevier Ltd. This is an open access article under the CC BY license (<http://creativecommons.org/licenses/by/4.0/>).

molecular ability to acquire an electric dipole moment when subjected to an electric field [2,3,6–8]. Aromatics are, furthermore, compounds with single/small benzene rings, having a low volume of heteroatoms, such as sulfur, and an average aromatic ring number of 2.6 [2,3,6–8]. Resins are polar aromatic molecules, speculated to have an aromatic core of 2–4 fused rings with a structure and chemical similarities to the asphaltenes [2,3,6–8].

Petroleum derivatives such as crude oil, heavy oils, and bitumen can be classified as a combination of various ratios of the 4 SARA fractions. In SARA fractions, asphaltenes interact with resins (that act as surfactants) to form stable asphaltene aggregates and saturates is the solvent phase in which the asphaltene aggregates are dispersed [3,9–11]. The overall stability of the asphaltene aggregates is associated with external and internal factors such as interaction strength, solubility parameter, evolution of violates, and the ratio of other molecules to asphaltenes [1].

To improve its performance and service life and increase its load-bearing capacity as well as reduce its maintenance cost, bitumen is often modified with nanoparticles, due to their high surface area and ability to tailor their properties [12]. One such group of nanoparticles is graphene and its derivatives [13–15]. Compared to other nanoparticles, graphene has superior material properties (such as high thermal conductivity, electrical conductivity, and excellent gas barrier properties), it is also optically transparent, flexible, and it is possible to tailor its shape [16,17].

The incorporation technique of graphene derivatives, i.e., the method by which it is delivered into bitumen, plays a significant role in how the nanoparticle will contribute to the properties of bitumen. There are two primary methods for this, directly or indirectly incorporation [13,15]. The indirect method includes incorporating graphene derivatives into a polymer carrier, which is pelletized and thereafter dispersed in the bulk of bitumen [18]. By this approach, the graphene derivatives only indirectly contribute to the properties of bitumen. Furthermore, the polymer carrier can have negative effects on some desired properties, such as the thermal conductivity, and therefore it of interest to also find methods to directly introducing graphene derivatives into bitumen.

There are numerous publications in the last years [13,15,19–30] that discuss the direct incorporation of graphene and graphene derivatives such as graphene oxide (GO), and reduced graphene oxide (rGO) into bitumen, and claim an improvement of its viscoelastic, thermal, or oxidative properties. However, by investigating the impact graphene derivatives have on asphaltenes (and consequently on bitumen) we have previously shown that such conclusions are false positive [4]. From our previous experimental study, we could conclude that such positive results are a consequence of a macroscopic research perspective in combination with studies of so highly viscous systems that detrimental destabilization and phase separation was not observed during the studied timescale. From our study on a more diluted system, it was furthermore evident that asphaltene aggregates (asphaltene and resins) permanently adsorb onto the surface of GO to form agglomerates, which has a negative influence on the colloidal stability and leading to phase separation [4]. This is detrimental because asphaltene aggregates are critical to the function of bitumen, as these non-isodiametric aggregates contribute to properties like stability, viscosity, viscoelasticity, and adhesion [1]. The adsorption occurs due to hydrogen bonding and/or acid-base interactions between the oxygenated groups on GO and the heteroatomic functional groups on resins and asphaltenes, and  $\pi$ - $\pi$  interactions between the polyaromatic structures of the asphaltene and GO [4]. Thus, there are several challenges of directly incorporating graphene derivatives into bitumen. In fact, there has been no method to successfully incorporate graphene into bitumen (i.e., without causing phase separation and precipitation) without using covalent functionalization of graphene, which instead tends to destroy many of the desired electronic properties of graphene by converting the highly conducting sp<sup>2</sup>-hybridized state to the substantially less conducting sp<sup>3</sup>-hybridized state [16]. This implies that there is a lack of methods to maintain the

desired properties of graphene at the same time as it is incorporated into bitumen without destabilizing effects. In this article we present such a method, called the molecular wedging (MW) method, thereby filling the knowledge gap and providing a ‘roadmap’ to how graphene should be incorporated into bitumen without causing destabilizing effects. We show that the incorporation of functionalized graphene by the MW-method is not only possible without destabilize the system, but also that the stabilization of the system is enhanced compared to the system without incorporated graphene. This, in turn, leads to a longer service life for bitumen and its applications, such as asphalt for roads.

## 2. Material and methods

In this study, we developed a bitumen model system, i.e., a synthetic SARA fraction, called the MW-graphene system, to be able to study the interaction between the graphene derivative and the asphaltene aggregates in more detail.

### 2.1. Materials and sample preparations

For this study, M-grade XGNP graphene from XGScience, consisting of nanoplatelets with an average diameter of 25  $\mu$ m, a surface area of 120–160 m<sup>2</sup>g<sup>−1</sup>, a thickness of 6–8 nm and a density of 2.2 kgcm<sup>−3</sup> was used. Four different MW-graphene systems were developed, each functionalized with one of the aromatic pyrene-based molecules: 1-pyreneboronic acid (PBrA), 1-pyrene-butyric acid (PBA), 1-pyrenesulfonic acid (PSA) or 1-aminopyrene (PAM). Dodecylbenzene sulfonic acid (DBSA), PBrA, PBA, PAM, PSA, methanol, toluene (90%), and paraffin oil were all purchased from Sigma Aldrich. The asphaltene nanoaggregates were extracted from bitumen, as described below.

### 2.2. Synthesis of MW-graphene

As mentioned above, to effectively use a graphene derivative in bitumen, it must be functionalized to avoid detrimental agglomeration, destabilization, and precipitation. In this study we used non-covalent functionalization, where molecules are attached on graphene through hydrogen bonding, electrostatic interactions, or  $\pi$ - $\pi$  interaction [31,32]. More specific, we used the MW-method [33] to obtain an effective interaction between graphene and the functional groups as well as between the functional groups and the asphaltene aggregates.

For each MW-graphene, 100 mg of graphene was dispersed in 50 ml methanol and sonicated for 1 hour. Thereafter the desired aromatic molecule (PBrA, PBA, PAM, or PSA), was added to the solution and further sonicated for an hour. After this, 200 ml of double-distilled de-ionized water was added, and further sonicated for 24 hours. Thereafter the solution was centrifuged. The precipitate was decanted and redispersed in de-ionized water. The redispersed solution was further sonicated for 45 minutes, filtered, and rinsed and thereafter the material was vacuum-dried.

4 samples were prepared: PBrA-graphene, PBA-graphene, PSA-graphene and PAM-graphene. The chemical structure of each of the MW-graphenes are presented in Fig. 1. As shown, the aromatic molecule has a base consisting of pyrene with an heteroatomic functional group (hereafter called tether) bound to the pyrene. During functionalization, the pyrene base of the aromatic molecule is adsorbed onto graphene whereas the functional group extending from the surface. The different steps of the synthesis are schematically illustrated in Fig. 2.

### 2.3. Extraction of the asphaltene

The asphaltene phase was extracted from bitumen. Before extraction, the asphaltene content in bitumen was increased by the rolling thin-film oven test setup (RTFOT) [34]. The extraction of asphaltene was performed according to the American Society for Testing and Materials (ASTM) D-2007–80 standard. Firstly, n-heptane was added in a ratio of

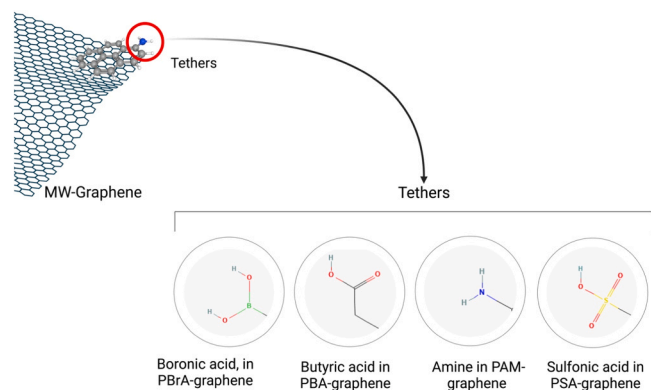


**Fig. 1.** The four MW-graphenes and the molecules present in the respective tethers, i.e., the heteroatomic functional groups.

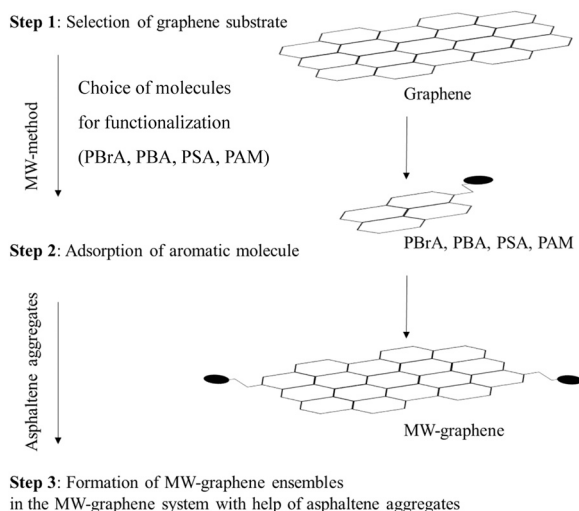


**Fig. 2.** Illustration of the functionalization of MW-graphene with the different steps involved in the production of the MW-graphene ensemble.

100 ml to 1 g of bitumen. This solution was then transferred in a flask and placed in an oil bath on a heating plate. A Dimroth reflux condenser with a connected water supply was placed on top of the flask. Then the entire setup was sealed using a lab clamp. The bitumen solution was then heated to 95 °C and steered for 1 hour before it was turned off. The solution was thereafter centrifuged and decanted. The precipitate, i.e., the asphaltene, was then air-dried for 24 hours to ensure that the extracted material was completely dry of any solvent before it was redispersed in toluene. The extracted, and thereafter redispersed, asphaltene is generally in the form of asphaltene nanoaggregates [35–37]. Asphaltene nanoaggregate is the low energy state of asphaltene, where stacks of less than 10 sheets of asphaltene stack together [38].

#### 2.4. Synthesis of the MW-graphene systems

Firstly, a colloidal precursor was prepared by dispersing 0.5 ml of DBSA in 10 ml of paraffin oil ( $\approx 5$  wt%). For the preparation of asphaltene aggregates, 5 mg of asphaltene nanoaggregates was dispersed in 5 ml of the colloidal precursor and sonicated. To prepare the MW-graphene systems, a volume fraction of 10 wt% of the desired MW-graphene was introduced into the asphaltene aggregate system and sonicated for 10 minutes. A detailed description of the involved steps and weight fractions of the different molecules is given in our previous work [33]. Each MW-graphene system describes a model bitumen, i.e.,

represents bitumen with the corresponding MW-graphene ensemble present in it. The preparation steps are presented in Fig. 2 and the names and chemistry during the functionalization steps of all the MW-graphene systems are provided in Table 1.

#### 2.5. Sample preparation for experimental measurements

To investigate the stability of the MW-graphene systems over time, one part of each MW-graphene system was stored in glass vials for long-term visual observation, while the other part of each batch was used to study their precipitation rate (over 7 days) by microscopy measurements. Microscopy was conducted using the supernatant from the cuvettes, which should be the most sensitive part for evaluation of the stability (precipitation) of the systems over time. It should here be emphasized that there is a great advantage of using our model systems instead of bitumen. For instance, if bitumen had been used the samples had not been optically transparent and therefore not been possible to study by microscopy. Furthermore, the present model systems have lower viscosity than bitumen, which is essential (as mentioned above) for being able to elucidate the colloidal stability of the studied systems and related graphene incorporated bitumen. In addition, the model systems are chemically simplified compared to corresponding systems based on bitumen and the role of the functionalization strategy for the colloidal stability is therefore easier to interpret and understand.

#### 2.6. X-ray photoelectron spectroscopy

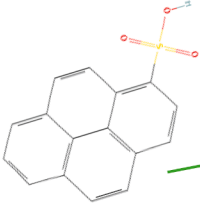
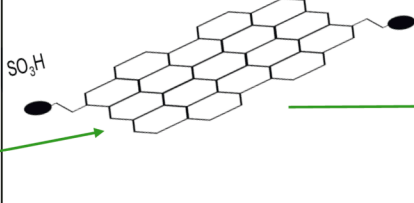
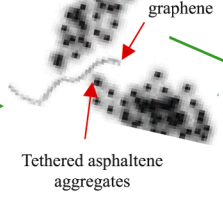

The X-ray photoelectron spectroscopy (XPS) measurements were performed with a PHI5000 VersaProbe III – Scanning XPS Microprobe at room temperature around 20 °C. The instrument was equipped with a monochromatic AlK $\alpha$  x-ray source with the photon energy at 1486.6 eV and the beam diameter set at 100  $\mu$ m. Since all investigated samples are nonconductive, both argon ion gun (+ve) and electron neutralizer (-ve) were running during the measurements to achieve the dual charge compensation. Binding energy scale of the instrument was calibrated and aligned with the core level spectra of gold (Au4f $_{7/2}$  = 83.96 eV), silver (Ag3d $_{5/2}$  = 368.21 eV) and copper (Cu2p $_{3/2}$  = 932.62 eV), respectively, in accordance with [39]. The energy resolution of a measured core level peak is 0.63 eV, with reference to the full width at half maximum (FWHM) of a Ag3d $_{5/2}$  peak measured from a sputter-cleaned silver foil by a 100  $\mu$ m X-ray beam. To gain an overview about the surface chemical composition, survey spectrum was acquired in an energy range between 0.0 and 1250.0 eV with a step size of 1.0 eV, under the pass energy of 280.0 eV. Narrow scans were followed in the selected energy regions to analyze the chemical state(s) of the elements of interest. During narrow scans, pass energy was reduced to 26.0 eV and the step size became 0.10 eV for most of the elements, and even 0.05 eV for carbon, in order to acquire the refined features in different spectra.

Data analysis of the XPS results was carried out in PHI MultiPak software (Version 9.7.0.1). Prior to quantitative analysis, Shirley background was applied to the spectra to subtract the signal contribution from the scattering of low energy electrons [40]. To aid the qualitative analysis, the main peak in the core level C1s spectrum was first aligned at 284.5 eV, with reference to the sp $^2$ -hybridized carbon state in graphene [41–43]. Then, an asymmetric Gauss-Lorentzian function was applied to fit this specific carbon state, whilst all the others were fitted with the symmetric Gauss-Lorentzian function [40–47].

Since XPS is a highly sensitive surface chemistry technique, a sample must be cleaned off from any surface contamination. Before measurement, the material was cleaned and sonicated in methanol. Methanol was chosen because it can evaporate after deposition and will not bind onto the graphene surface, unlike water. After sonication, the MW-graphene was deposited on a silicon wafer and dried to remove any residual methanol. By this, a thin layer of the material was deposited on the surface of the wafer.

**Table 1**

An illustration containing the names of the different aromatic molecules, the chemical structure of the tethers, their corresponding MW-graphenes and the MW-graphene ensembles formed by the functionalized graphene, and the final sample for a visual understanding.

Samples	Aromatic molecule	Tether	Graphene species used	MW-graphene (Functionalized graphene)	MW-graphene ensemble (after interaction with asphaltene aggregates)	MW-graphene system
	PBrA	Boronic acid	Graphene	PBrA-graphene	PBrA-graphene ensemble	PBrA-graphene system
	PBA	Butyric acid	Graphene	PBA-graphene	PBA-graphene ensemble	PBA-graphene system
	PSA	Sulfonic acid	Graphene	PSA-graphene	PSA-graphene ensemble	PSA-graphene system
	PAM	Amine	Graphene	PAM-graphene	PAM-graphene ensemble	PAM-graphene system
Definitions	The molecules used to develop different MW-graphenes	The heteroatomic functional group present on the aromatic molecule	The graphene received from the supplier	Graphene that was functionalized by MW-method and tethers on its surface	Novel hybrid structure with MW-graphene with tethered asphaltene aggregates, attached to it via the tethers, and is stable in saturates	A simplified model system used in this study. It is equivalent to MW-graphene incorporated in bitumen. It contains the MW-graphene ensemble and all possible structures formed by the interaction between the different chemical constituents used to develop the system
Illustrations						
	PSA		PSA-graphene		PSA-graphene ensemble	PSA-graphene system

## 2.7. Transmission light microscopy

Transmission light microscopy (TLM) with bright field, phase contrast and polarized light modes was performed using an Olympus BX53 microscope. For each measurement, a droplet of the system (taken from the supernatant) was placed on a glass slide. Also these measurements were performed at room temperature, i.e., a temperature of about 20 °C, and at magnifications of 10X, 20X and 40X.

## 3. Results

### 3.1. Functionalization verification of MW-graphenes

The functionalization of the MW-graphenes was verified by XPS. The survey spectra in Fig. 3 shows that carbon (C) and oxygen (O) are the most abundant elements in pure graphene and all the MW-graphenes, with the total content above 97.0 at.%. By contrast, the key element from individual functional group contributes only 1.0 at.% or less, including boron (B) in PBrA-graphene, sulfur (S) in PSA-graphene and

nitrogen (N) in PAM-graphene. In addition, silicon (Si) content that contributes from the silicon wafer is determined from PSA- and PAM-graphenes.

Selected energy spectra including B1s, C1s, N1s, O1s, and S2p, based on the ingredients in pure graphene and the individual MW-graphenes, are summarized and plotted in Fig. 4. As a reference material in this study, the C1s spectrum of pure graphene exhibits a main peak locating at 284.5 eV, which corresponds to the sp<sup>2</sup>-hybridized carbon. Three oxygenated carbons are determined at 286.5 eV, 288.0 eV and 289.5 eV, respectively, and correspond to the epoxide (C-O-C), carbonyl (C=O) and carboxylic (COO<sup>-</sup>) groups. Though the oxygenated types contribute weakly in the C1s spectrum, the carbonyl and epoxide groups are clearly determined in the O1s spectrum at 531.8 eV and 532.9 eV, respectively, in the graphene measurement. The oxygenated carbon peaks are a result of the chemical exfoliation of graphite into graphene, which can result in residual species. Besides that, the fitted peak in C1s at 291.5 eV is the characteristic feature of a π-π\* peak for the proof of graphene structure [41–43,45–47], and the fitted peak above 535.0 eV in O1s refers to water (H<sub>2</sub>O) or the adhered moisture [41]. With regards to C1s and O1s



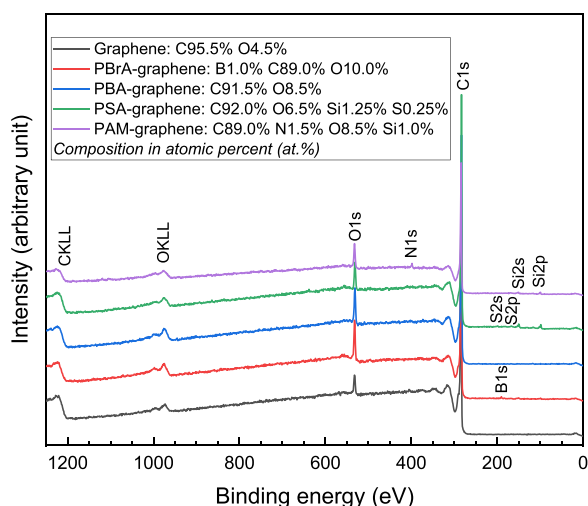


Fig. 3. XPS survey spectra of pure graphene and the four MW-graphenes.

spectra, all the other MW-graphenes are basically sharing the same characteristic features as in pure graphene, as shown in the two stacked spectra in Figs. 4(a) and 4(b), just the proportion of different oxygenated states vary from one to another (Table 2).

The graphene functionalization by a 1-pyrene-boronic acid molecule gives rise to a boronic peak in the interval 188.0–192.0 eV in the B1s spectrum [48]. In PBrA-graphene, the boronic acid is bonded to one carbon and two oxygen atoms (see Fig. 1), and the B1s spectrum provides evidence for the expected B-C bond at 191.0 eV (Fig. 4c(ii)), and the corresponding position in the C1s spectrum is at 283.5 eV [42]. The C1s spectrum of PBA-graphene, i.e., graphene functionalized by 1-pyrene-butyric acid, displays five deconvoluted peaks (Fig. 4a(iii)). When compare this spectrum with that of pure graphene, it is observed that the functionalization by PBA gives rise the contribution from the oxygenated carbons, especially the carboxylic group at 289.5 eV (Table 2) [49]. As compared to the O1s in graphene, the proportion of carbonyl group increases upon functionalization in the system and the carboxylic group

that locates at 533.4 eV is uniquely determined as compared to the others (Fig. 4b(iii)) and Table 2). The S2p spectrum of PSA-graphene shows the presence of an unusual symmetric peak for a proper S2p profile. It is because this region is overlapping with the Si plasmon peak, and the Si content is more abundant than sulfur (see Fig. 3). For that, the peak deconvolution is carried out in 2 steps. First, a symmetric Gauss-Lorentzian function is fitted for the plasmon contribution. Then, rest of the region is fitted with a spin-orbit doublet of S2p<sub>3/2</sub> and S2p<sub>1/2</sub> [50] (Fig. 4c(iv)). The fitted position for S2p<sub>3/2</sub> is around 168.0 eV, and is expected for an oxygenated sulfur species, as in R-SO<sub>3</sub>H in the functional group [44,47]. The measurement of PAM-graphene shows that a N1s peak is observed at 399.3 eV (see Fig. 4c(v)), indicating the presence of the expected pyrrolic bond between the PAM molecule and graphene [49]. Thus, the performed XPS measurements confirm a successful functionalization of the four molecules onto graphene.

The difference between a successfully and an unsuccessfully functionalized graphene derivative is dramatic. Fig. 5 (A) shows our previous results for GO [4]. In the figure, the agglomerated structures, which are due to the irreversible adsorption of asphaltenes on the surface of GO, are clearly shown. These structures do not display any long-range order and have a size distribution ranging from a few microns to up to 50 microns [4]. The ring around the structures, indicated by an arrow in the figure, is the boundary between the phase separated GO-asphaltene structure and saturates. Thus, whereas the incorporation of GO (i.e., graphene oxide) leads to a rapid precipitation [4], functionalization with a pyrene-based aromatic molecule with an heteroatomic functional group like PBA, Fig. 5 (B), gives rise to a successful interaction between asphaltene aggregates and graphene derivatives, resulting in a stable graphene-asphaltene network structure. Thus, in the latter case, the interaction between the MW-graphene and the asphaltene aggregates causes the MW-graphene to act as a nucleation site around which the asphaltene aggregates form large network structures [33].

### 3.2. Formation and evolution of the MW-graphene systems

The stability of the four MW-graphene systems over time was investigated by TLM. Fig. 6 and figure S2 of SI shows that MW-graphene ensembles (shown as black particles in Fig. 5, for zoom-in images, see

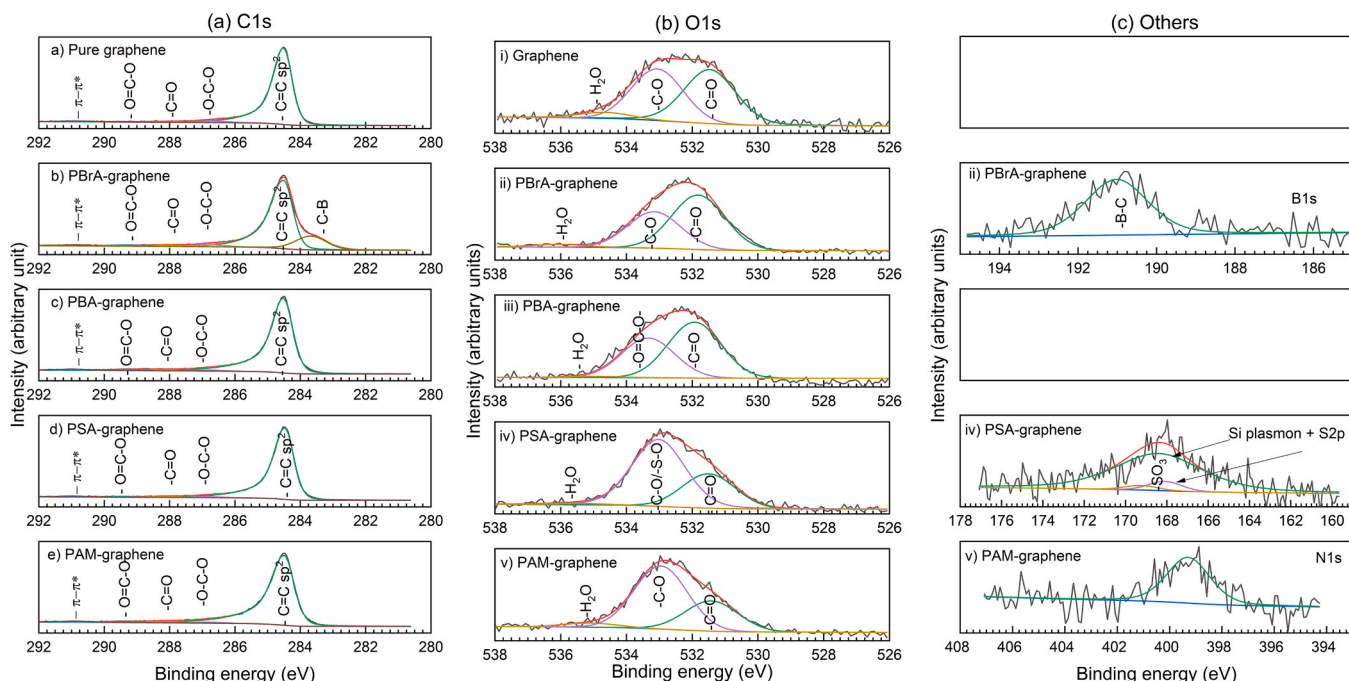
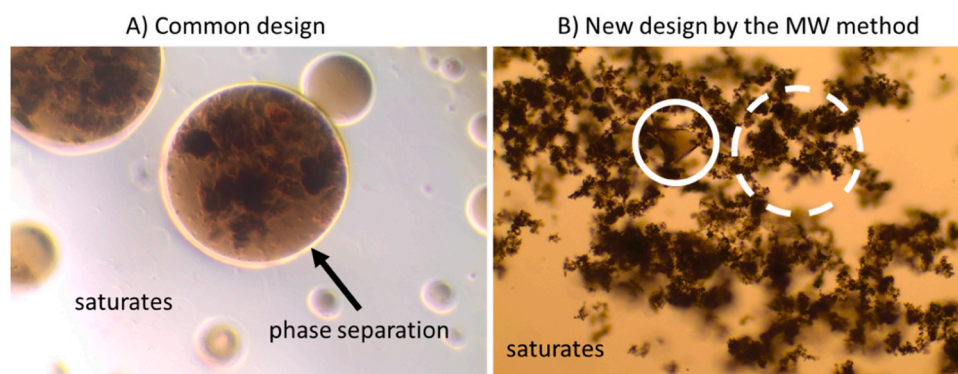


Fig. 4. XPS narrow scanned spectra of (a) C1s, (b) O1s, and (c) others including B1s, N1s, and S2p from the (i) graphene, (ii) PBrA-graphene, (iii) PBA-graphene, (iv) PSA-graphene and (v) PAM-graphene. The spectra provide clear evidence that the functionalization was successful for each of the MW-graphenes.

**Table 2**

A summary showing the potential chemical states and their corresponding binding energy positions of individual elements in pure graphene and the MW-graphenes based on references [41–47], as well as their corresponding contribution in the composition.

Element (Peak)	Chemical state	Binding Energy	Graphene	PBrA-graphene	PBA-graphene	PSA-graphene	PAM-graphene
Boron (B1s)	B-C	191.0 eV [52]		1.0 at. %			
Carbon (C1s)	C-B	284.2 eV [42]		15.8 at. %			
	sp <sup>2</sup> -hybridized (C=C)	284.5 eV [41–43]	90.0 at. %	66.6 at. %	85.7 at. %	86.7 at. %	83.5 at. %
	O-C-O (Epoxide)	286.1–286.8 eV [41,42,45–47]	2.3 at. %	2.2 at. %	1.4 at. %	1.5 at. %	1.2 at. %
	C=O (Carbonyl)	287.5–288.5 eV [45–47]	1.0 at. %	1.6 at. %	1.3 at. %	1.3 at. %	1.6 at. %
	O=C-O <sup>-</sup> (Carboxylic)	288.5–289.0 eV [46,47]	0.9 at. %	1.5 at. %	1.6 at. %	1.1 at. %	1.3 at. %
	$\pi$ - $\pi^*$ (satellite bonds in the p <sub>z</sub> -orbital)	289.5–291.0 eV [41–43]	1.3 at. %	1.3 at. %	1.5 at. %	1.4 at. %	1.4 at. %
Nitrogen (N1s)	R-NH (Pyrrolic)	399.3 eV [45]					1.5 at. %
Oxygen (O1s)	O=C (Carbonyl)	531.8 eV [41]	2.25 at. %	6.0 at. %	5.0 at. %	2.0 at. %	2.5 at. %
	O-C (Epoxide)	532.7 eV [41]	2.0 at. %	4.0 at. %		4.5 at. %	5.5 at. %
	O=C-O <sup>-</sup> (Carboxylic)	533.4 eV [41]			3.5 at. %		
	H <sub>2</sub> O (Water or moisture)	535.1 eV [41]	0.25 at. %				0.5 at. %
Sulfur (S2p <sub>3/2</sub> )	R-SO <sub>3</sub> H (Sulfonate)	168.2 eV [44]				0.25 at. %	



**Fig. 5.** A) The common design i.e., asphaltene aggregates (asphaltene and saturates/resin) and graphene oxide (GO) results in phase separation. B) MW-graphene with its functional group results in stable asphaltene aggregates. The solid line shows the MW-graphene and the dashed line the network of asphaltene aggregates tethered to the MW-graphene.

figure S1 of SI) are present in all the four systems at day 1 (i.e., 1 day after preparation). This ability to form ensembles in the presence of asphaltene aggregates indicates that the only requirement for this process to occur is the presence of tethers on the surface of MW-graphene. Thus, graphene can be stabilized in bitumen if the tethers are phase compatible with the asphaltene aggregates. However, significant variations between the systems are observed already one day later. For the PBrA-graphene system, the TLM image reveals two observations. Firstly, larger particles are observed, which likely are PBrA-graphene ensembles clustered with "untethered" asphaltene aggregates, similar to what was observed in our prior work [33]. Secondly, the sample displayed a reduction in observable MW-graphene ensembles compared to day 1. In contrast, the PBA-graphene and PSA-graphene systems show no signs of such agglomeration. However, both samples display a minor reduction in the number of observable MW-graphene ensembles compared to day 1, indicating some precipitation. The PAM-graphene system exhibits a large macroscopic structure due to substantial agglomeration. Additionally, several PAM-graphene ensembles are observed alongside with this macroscopic structure.

By day 5, the clustered MW-graphene ensembles observed earlier are no longer visible in any of the four MW-graphene systems. Instead, in all four MW-graphene systems the MW-graphene ensembles have clustered together and formed phase-separated structures with well-defined boundaries. This is most pronounced for the PBrA-graphene system, but similar agglomerates are also seen for the three other systems. Overall, it is clear that the black particles, i.e., single MW-graphene ensembles, observed at day 1 are no longer visible, but instead different agglomerates are observed.

After a week, the PBrA-graphene system exhibits an almost complete precipitation of the ensembles in the supernatant, as shown in Fig. 5. However, a few well-defined PBA-graphene agglomerates are observed in the PBA-graphene system, although larger agglomerates cannot be found. The PSA-graphene system still has some agglomerates present, but they are significantly smaller than those observed on day 5. The PAM-graphene system has numerous agglomerates present, similar to those observed in the PBrA-graphene system on day 2, indicating a low degree of precipitation. Thus, from the TLM images in Fig. 6 it can be concluded that the PAM-graphene system is the most stable MW-graphene system over time, followed by PSA-graphene and PBA-graphene, with PBrA-graphene as the less stable system.

The reason for the stability variations of the MW-graphenes is not clear, but it can most likely be attributed to the chemical nature (acidity) of the tethers and their potential interaction with asphaltene aggregates. In addition, the chemistry of asphaltene is complex, and the mechanism that leads to the formation of asphaltene aggregates is not fully understood [3,38,51–53]. Therefore, assuming that all four MW-graphene ensembles engage in the same stabilization mechanism with the asphaltene aggregates might be an oversimplification. In fact, many studies of surfactants used in bitumen show that highly acidic surfactants form a strong bond with asphaltene, and thus act as excellent surfactants [54–60]. Thus, if such bonds are formed, the acid will be irreversibly attached to the asphaltene.

The predicted pKa values of the molecules used for functionalization are PBrA (8.53) > PBA (4.76) > PAM (4.32) > PSA (2.8) [61,62]. While the acidity of the tethers can be modified due to the presence of other polar molecules and the delocalization of electrons due to the carbon

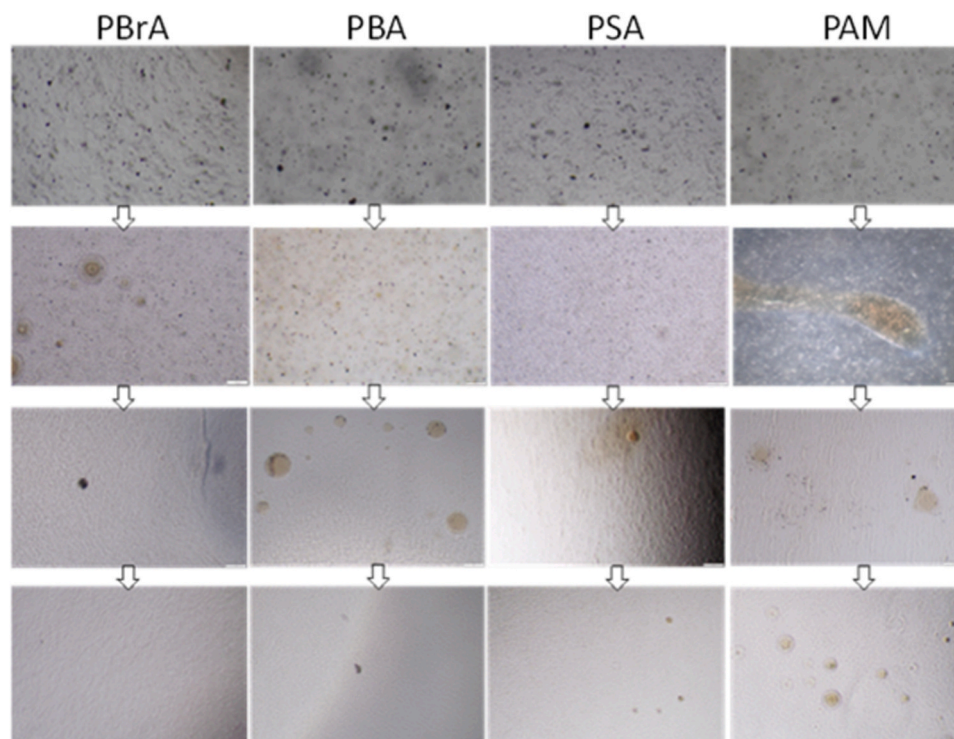


**Fig. 6.** TLM images of the PBrA-, PBA-, PSA-, and PAM- graphene ensemble systems at day 1 (top row), day 2, day 5 and day 7 (bottom row) after preparation. Amplified images of the systems are shown in Figs. S3-S6 of SI (S3 shows the systems at day 1 and S6 the systems at day 7).

structure of graphene, we speculate that the pKa-values are correlated with the observed stability of their corresponding MW-graphene ensembles. Hence, although the level of stability likely depends on several properties of the functional group, the pKa-value seems to be a key parameter, and there might be a threshold acidity/pKa-value required to form a stable MW-graphene system. However, it should be noted that this has to be investigated in detail before conclusions can be made, and this has not been our focus in this study where we only have tried to find a method to incorporate graphene into bitumen without negatively affecting the colloidal stability of the asphaltene aggregate system.

### 3.3. Long-term stability

The stability ranking of the four MW-graphene systems obtained by the microscopy investigation over 7 days after preparation is further supported by a direct visual inspection of the samples after a storage time of 6 months, see Fig. 7. The figure shows that the PBrA-graphene system is the least stable and that it exhibits about the same degree of precipitation as the pure asphaltene aggregate system. The PSA-graphene and PAM-graphene systems, on the other hand, seem to be the most stable as no clear precipitation is visible, even after this long storage time. The PBA-graphene system shows an intermediate stability which is substantially higher than that for the pure asphaltene aggregate system and the PBrA-graphene system, but also clearly lower than for the PSA-graphene and PAM-graphene systems. Thus, as shown by the visual inspection after 6 months of storage, it is clear that by using the MW method it has been possible to not only maintain but also enhance the colloidal stability of the asphaltene aggregate system with at least three of the four functional groups used in this study.

## 4. Discussion

From the Introduction section it is evident that agglomeration of both graphene derivatives and asphaltene is inevitable without appropriate functionalization of the graphene. Thus, to successfully utilize

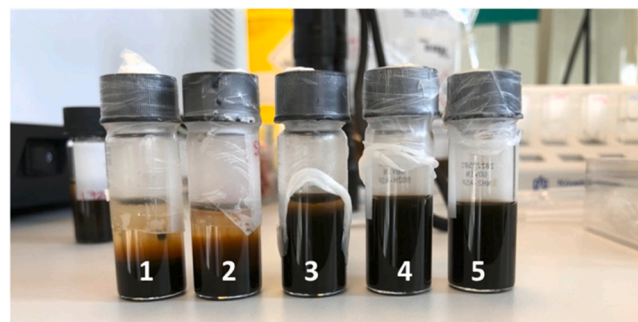


**Fig. 7.** Visual observation of the MW-graphene ensemble systems after a storage time of 6 month in comparison with the pure asphaltene aggregate systems. From left to right in the figure, the vials containing (1) the asphaltene aggregate system, the (2) PBrA-, (3) PBA-, (4) PSA-, and (5) PAM-graphene systems, respectively.

graphene in bitumen, the nanoparticles must be chemically modified (functionalized), and in this study the following design criteria were identified to be crucial for utilizing the potential of graphene derivatives in bitumen:

1. Accounting for the physical and chemical characteristics of graphene derivatives.
2. Accounting for the stability of asphaltene aggregates in bitumen.
3. Accounting for physical and chemical stability of graphene in bitumen.
4. Accounting for environmental impact of modifying bitumen.



#### 4.1. Accounting for the physical and chemical characteristics of graphene derivatives

The physical and chemical characteristics of graphene and graphene derivatives significantly impact its applicability in bitumen. For instance, in applications where thermal conductivity, electrical conductivity, and smart sensing are of importance for high performance, graphene must be maintained in its high fraction of sp<sup>2</sup>-hybridized state [16]. In an sp<sup>2</sup>-hybridized state, the s, p<sub>x</sub>, and p<sub>y</sub> orbitals share electrons with the three nearest atoms, thereby forming  $\sigma$ -bonds in-plane. The remaining electrons of the carbon atoms occupy the outer shell of the p<sub>z</sub> orbital, i.e., oriented perpendicularly to the plane. This orbital hybridization results in the formation of two half-filled bands ( $\pi$ - $\pi^*$ ) of free-moving electrons [16,18,63]. The free electrons give graphene its metallic nature (with thermal and electrical conductivities) [16,18,63]. Thus, if the surface chemistry of graphene, during functionalization, is transformed to another hybridized state than sp<sup>2</sup>, as discussed below in the case of covalent functionalization, the number of free-moving electrons are reduced [16], and consequentially, the conductivity of graphene is decreased.

In our previous study, it was identified that covalent functionalization could result in a transformation of more than 50% of the surface into an sp<sup>3</sup> hybridized state [4], which thus significantly impacts the metallic properties of graphene. During covalent functionalization, a chemical bond is created between the graphene surface and the functional group. Since graphene itself is inert, it has to be transformed into GO, which affects the hybridization, for the formation of a covalent bond to the functional group. Consequently, a large fraction of the graphene surface is transformed from an sp<sup>2</sup> to an sp<sup>3</sup> hybridized state. This functionalization strategy is therefore counterproductive as graphene is of interest for bitumen modification due to superior material properties related to the sp<sup>2</sup> hybridization.

In addition, our previous investigation revealed that graphene derivatives such as GO have a direct detrimental effect on the properties of bitumen [4] due to the impact of GO on the asphaltene aggregates (see Fig. 4). The primary interaction that leads to the detrimental effect is the acid-base interaction between the oxygenated groups on GO, such as the hydroxyl, epoxide, and ketones, and the heteroatomic functional groups on resins and the asphaltenes (formed by nitrogen, oxygen, and sulfur atoms). This interaction leads to that asphaltenes and resins adsorb onto the surface of GO, which has a huge negative effect on the colloidal stability. Therefore, a crucial step in the functionalization of the surface of a graphene derivative is to avoid destabilization of the asphaltene aggregates.

Non-covalently functionalization, on the other hand, involves electrostatic interactions between two molecules, such as  $\pi$ -effects, van der Waals forces, and hydrophobic effects, which does not affect the surface hybridization as seen in Table 1. Thus, by non-covalently functionalization, the graphene surface remains in approximately the same fraction of sp<sup>2</sup> hybridized state as the nonfunctionalized graphene and retains thereby its superior material properties.

#### 4.2. Accounting for stability of asphaltene aggregates in bitumen

Structural studies of asphaltene aggregates show that they have a broad stability range that is influenced by factors such as temperature, pressure, orientations, order, and concentration [1,3,10]. As confirmed in this study, the addition of nanoparticles to bitumen or modifications of its existing aggregate structure will directly impact the stability [1,3,10]. For instance, if graphene derivatives are partly adsorbed in two different clusters, it could lead to bridging between the clusters, causing agglomeration despite the existence of electrical repulsion potential [1,3,10]. Thus, functionalization of graphene derivatives that impact the stability of asphaltene aggregates must be avoided due to the risk of flocculation, deposition, and sedimentation/precipitation. However, if the graphene derivatives are functionalized with a pyrene based organic

acid group (e.g., carboxylic acid, sulfonic acid, or boronic acid) or an amine group, as in our case, then the asphaltene aggregates will not be involved in an electron donor-receiver with the graphene derivatives [4]. Thereby the asphaltene aggregates will remain stable.

#### 4.3. Accounting for physical and chemical stability of graphene in bitumen

To utilize the potential of graphene for bitumen applications it must be well dispersed. If a dispersion is not achieved, the graphene derivatives will precipitate and thus not contribute to the properties of bitumen. Since graphene does not naturally disperse in saturates, it will have to be stabilized by adding functional groups on its surface [64]. A further challenge to incorporate graphene derivatives into bitumen is that different sources of bitumen may have extremely varying properties [65]. It is also a common industrial practice to mix different sources of bitumen to obtain desired viscoelastic properties for specific applications. This implies that the final composition will have a unique chemical structure and composition, and thereby also a unique SARA fraction that is not representative of the crude sources [1,11,65]. Due to this variation and uncertainty in bitumen chemistry, the introduced graphene derivative must stabilize itself at all service and processing conditions. In this paper we present the first non-covalent functionalization method to achieve this. By functionalizing graphene with suitable molecules, such as PSA and PAM, we are able to produce a symbiotic and simultaneous stabilization between graphene derivatives and asphaltene aggregates. Thus, we make use of the intrinsic stable asphaltene aggregates to stabilize itself and the incorporated graphene derivatives simultaneously. This is key finding for the possibility of incorporating graphene into bitumen and bitumen containing materials without destabilizing the colloidal structure of bitumen and/or losing the desired electronic properties of graphene.

#### 4.4. Accounting for environmental impact of modifying bitumen

Bitumen is used in millions of tons yearly and the environmental footprint of modifying such an extensively used material is significant and must be accounted for [66]. Any modifying agent (such as nanoparticles) that are developed to be incorporated into bitumen must also be manufactured in millions of tons [66]. If the nanoparticle is chemically demanding to manufacture, it will have a net negative impact on the environment. For example, if a covalent functionalization technique is used to synthesize the graphene functional group, the process uses a large amount of different chemicals [67]. In addition, for such a synthesis graphene has to be transformed into GO as an intermediate, which consumes large amounts of energy (20 GJ/Kg to 38 GJ/Kg depending on the route [68]). When this energy requirement is scaled up to the volumes of bitumen used annually, the evaluation of the final result must be compared against such values.

Additionally, if complex functional groups are used for the functionalization, the process may require multiple chemicals. These chemicals, or the byproduct of the reactions during the functionalization, can be toxic [69]. This implies that if graphene derivatives are produced using unsustainable strategies, millions of tons of toxic chemicals will have to be utilized, causing a net negative impact on the environment. Thus, graphene derivatives must be modified using environmentally and economically conscious methods.

#### 4.5. Effective design strategy for modifying bitumen

From our studies it is clear that the MW method is the most promising strategy to functionalize graphene derivatives, such that it satisfies all the design criteria discussed above, when compared to other functionalization strategies [70]. Due to the polar nature of the MW-graphene, asphaltene aggregates interact with the functional groups, resulting in a stabilization of graphene in bitumen. Further, the

method is simple and requires only water and methanol as solvents, which both are recoverable at the end of the synthesis. In addition, utilizing asphaltene aggregates in stabilizing the MW-graphene eliminates the need for further functionalization of graphene to self-stabilize in bitumen. This is thus an environmentally friendly design strategy that saves millions of liters of harmful chemicals and time for synthesis. Hence, the non-covalent functionalization of graphene using the MW method and using asphaltene aggregates for the stabilization, is an excellent solution to modify bitumen in large-scale industrial applications in an environmentally conscious manner.

## 5. Conclusions

Bitumen is a material extensively used for the surface layer of roads around the world. Despite its usefulness and wide adoption, the material is also inefficient in conducting heat or providing multifunction. Due to this, many attempts have been made to modify its properties. One popular solution has been to use graphene as a modifier for improving material properties, such as viscoelasticity and thermal conductivity. However, we identified that the existing strategy does not improve the material properties but is rather detrimental to the properties of bitumen by causing agglomeration of graphene and asphaltene, leading to phase separation, destabilization, and precipitation. Thus, a new and sustainable strategy is needed to overcome these detrimental effects, and in this work a non-covalent functionalization technique called the molecular wedging (MW) method is presented to reach the desired colloidal stability of graphene incorporated bitumen. The method utilizes pre-existing and intrinsic stable asphaltene aggregates to stabilize itself and the incorporated graphene derivatives simultaneously. This method utilizes acid or amine end-functionalized pyrene molecules to functionalize graphene, and the MW-graphene retains in about the same fraction of its sp<sup>2</sup> hybridized as graphene (~80%), which preserves the desired properties of graphene. With this study we have thus shown that the MW method is an environmentally friendly solution to successfully incorporate graphene derivatives into bitumen for large-scale industrial applications. Thereby, we present the first successful strategy to incorporate graphene into bitumen without losing required colloidal stability (in fact, even increasing it) or negatively affecting the desired properties of graphene.

## Funding sources

The research was funded by the Norwegian Public Road Administration (Project ID: 2011 067932) and the Dept. of Architecture and Civil engineering, Chalmers University of Technology.

## Declaration of Competing Interest

The authors declare that they have no known competing financial interests or personal relationships that could have appeared to influence the work reported in this paper.

## Data Availability

All data is available upon request.

## Acknowledgment

We thank Govindan Induchoodan for help with sample preparations and measurements.

## Author contributions

The analysis of experimental data and writing of the manuscript is a joint work of the authors. All authors have given approval to the final version of the manuscript.

## Appendix A. Supporting information

Supplementary data associated with this article can be found in the online version at [doi:10.1016/j.nxmte.2024.100205](https://doi.org/10.1016/j.nxmte.2024.100205).

## References

- [1] Hunter, R., et al., *The Shell bitumen handbook*, 6th ed. 2015.
- [2] A. Neumann, et al., Investigation of aging processes in bitumen at the molecular level with high-resolution fourier-transform ion cyclotron mass spectrometry and two-dimensional gas chromatography mass spectrometry, *Energy Fuels* 34 (9) (2020) 10641–10654.
- [3] D. Lesueur, The colloidal structure of bitumen: consequences on the rheology and on the mechanisms of bitumen modification, *Adv. Colloid Interface Sci.* 145 (1–2) (2009) 42–82.
- [4] G. Induchoodan, H. Jansson, J. Swenson, Influence of graphene oxide on asphaltene nanoaggregates, *Colloids Surf. A: Physicochem. Eng. Asp.* 630 (2021) 13.
- [5] G.A. Olah, Á. Molnár, *Hydrocarbon Chemistry*, Wiley & Sons, 2003.
- [6] Y. Kostyukovich, et al., The investigation of the bitumen from ancient Greek amphora using FT ICR MS, H/D exchange and novel spectrum reduction approach, *J. Mass Spectrom.* 51 (6) (2016) 430–436.
- [7] F.J. Li, Y.H. Wang, K.C. Zhao, The hierarchical structure of bitumen of different aging states at the molecular level and nanoscale, *Fuel* 319 (2022) 16.
- [8] P. Kalhori, et al., Impact of crude oil components on acid sludge formation during well acidizing, *J. Pet. Sci. Eng.* 215 (2022) 10.
- [9] L.K. Alostad, et al., Investigating the Influence of n-Heptane versus n-Nonane upon the Extraction of Asphaltenes, *Energy Fuels* 36 (16) (2022) 8663–8673.
- [10] J.L. Bridot, D. Langevin, O.C. Mullins, Role of Asphaltene Origin in Its Adsorption at Oil-Water Interfaces, *Energy Fuels* 36 (16) (2022) 8749–8759.
- [11] M.R. Gray, M.L. Chacon-Patino, R.P. Rodgers, Structure-Reactivity Relationships for Petroleum Asphaltenes, *Energy Fuels* 36 (8) (2022) 4370–4380.
- [12] M. Porto, et al., Bitumen and bitumen modification: a review on latest advances, *Appl. Sci. -Basel* 9 (4) (2019) 35.
- [13] J. Crucho, et al., A review of nanomaterials' effect on mechanical performance and aging of asphalt mixtures, *Appl. Sci. -Basel* 9 (18) (2019) 31.
- [14] L. Moretti, et al., Mechanical characteristics of graphene nanoplatelets-modified asphalt mixes: a comparison with polymer- and not-modified asphalt mixes, *Materials* 14 (9) (2021) 17.
- [15] S.H. Wu, O. Tahri, State-of-art carbon and graphene family nanomaterials for asphalt modification, *Road. Mater. Pavement Des.* 22 (4) (2021) 735–756.
- [16] 2016, *Graphene oxide: Fundamentals and applications*.
- [17] A. Hazra, S. Basu, Graphene nanoribbon as potential on-chip interconnect material-a review, *C. -J. Carbon Res.* 4 (3) (2018) 27.
- [18] A.T. Lawal, Recent progress in graphene based polymer nanocomposites, *Cogent Chem.* 6 (1) (2020) 50.
- [19] F. Gulisano, et al., Piezoresistive behavior of electric arc furnace slag and graphene nanoplatelets asphalt mixtures for self-sensing pavements, *Autom. Constr.* 142 (2022) 13.
- [20] S.G. Jahromi, A. Khodaii, Effects of nanoclay on rheological properties of bitumen binder, *Constr. Build. Mater.* 23 (8) (2009) 2894–2904.
- [21] L. Luo, P.F. Liu, M. Oeser, A molecular dynamics simulation study on enhancement of thermal conductivity of bitumen by introduction of carbon nanotubes, *Constr. Build. Mater.* 353 (2022) 10.
- [22] Y.H. Wang, et al., Dispersion, compatibility, and rheological properties of graphene-modified asphalt binders, *Constr. Build. Mater.* 350 (2022) 14.
- [23] Y.Y. Wang, et al., Preparation and electrical properties of conductive asphalt concretes containing graphene and carbon fibers, *Constr. Build. Mater.* 318 (2022) 7.
- [24] Y.Y. Wang, et al., Evaluation of rheological and self-healing properties of asphalt modified microcapsules modified with graphene, *Constr. Build. Mater.* 357 (2022) 8.
- [25] X.M. Xie, et al., Evaluation of a cleaner de-icing production of bituminous material blending with graphene by electrothermal energy conversion, *J. Clean. Prod.* 274 (2020) 9.
- [26] Q.L. Yang, et al., Exploiting the synergetic effects of graphene and carbon nanotubes on the mechanical properties of bitumen composites, *Carbon* 172 (2021) 402–413.
- [27] F. Moreno-Navarro, et al., Mechanical and thermal properties of graphene modified asphalt binders, *Constr. Build. Mater.* 180 (2018) 265–274.
- [28] N.Z. Habib, et al., Use of graphene oxide as a bitume modifier: An innovative process optimization study, *Adv. Mater. Res.* 1105 (2015) 365–369.
- [29] C.Q. Fang, et al., Nanomaterials applied in asphalt modification: a review, *J. Mater. Sci. Technol.* 29 (7) (2013) 589–594.
- [30] H. Yao, et al., Rheological properties, low-temperature cracking resistance, and optical performance of exfoliated graphite nanoplatelets modified asphalt binder, *Constr. Build. Mater.* 113 (2016) 988–996.
- [31] V. Georgakilas, et al., Functionalization of Graphene: Covalent and Non-Covalent Approaches, Derivatives and Applications, *Chem. Rev.* 112 (11) (2012) 6156–6214.
- [32] N.A. Ismail, et al., Functionalization of graphene-based materials: Effective approach for enhancement of tribological performance as lubricant additives, *Diam. Relat. Mater.* 115 (2021) 12.

- [33] G. Induchoodan, et al., The critical role of asphaltene nanoaggregates in stabilizing functionalized graphene in crude oil derivatives, *Colloids Surf. A: Physicochem. Eng. Asp.* 660 (2023).
- [34] V.H. Kumar, S.N. Subbarao, Investigation of aging effect on asphalt binders using thin film and rolling thin film oven test, *Adv. Civ. Eng. Mater.* 8 (1) (2019) 637–654.
- [35] G. Andreatta, et al., Nanoaggregates and structure-function relations in asphaltenes, *Energy Fuels* 19 (4) (2005) 1282–1289.
- [36] L. Goual, et al., Cluster of asphaltene nanoaggregates by dc conductivity and centrifugation, *Energy Fuels* 28 (8) (2014) 5002–5013.
- [37] F. Mostowfi, et al., Asphaltene nanoaggregates studied by centrifugation, *Energy Fuels* 23 (3–4) (2009) 1194–1200.
- [38] F. Handle, et al., Tracking aging of bitumen and its saturate, aromatic, resin, and asphaltene fractions using high-field fourier transform ion cyclotron resonance mass spectrometry, *Energy Fuels* 31 (5) (2017) 4771–4779.
- [39] Standardization, I.O.f, ISO 15472:2010 Surface chemical analysis - X-ray photoelectron spectrometers - Calibration of energy scales.
- [40] ULVAC-PHI Inc, J., *PHI Multipak TM software manual (version 9)*. 2012: (<https://xp.slibrary.com/wp-content/uploads/-PHI-app-notes/XPS-Multipak-Manual.pdf>).
- [41] M. Brzhezinskaya, et al., One-pot functionalization of catalytically derived carbon nanostructures with heteroatoms for toxic-free environment, *Appl. Surf. Sci.* 590 (2022).
- [42] M. Sobaszek, et al., Highly Occupied Surface States at Deuterium-Grown Boron-Doped Diamond Interfaces for Efficient Photoelectrochemistry, *Small* 19 (26) (2023).
- [43] W.J. Xie, et al., Defects of clean graphene and sputtered graphite surfaces characterized by time-of-flight secondary ion mass spectrometry and X-ray photoelectron spectroscopy, *Carbon* 112 (2017) 192–200.
- [44] H. Baumann, L.D. Setiawan, D. Gribbin, Surface studies of keratin fibers and related model compounds using ESCA - Intermediate oxidation products of crystalline residues on keratin fiber surfaces and their hydrolytical stability, *Surf. Interface Anal.* 8 (5) (1986) 219–225.
- [45] M.K. Rabchinskii, et al., Unveiling a facile approach for large-scale synthesis of N-doped graphene with tuned electrical properties, *2d Mater.* 7 (4) (2020).
- [46] M.K. Rabchinskii, et al., Guiding graphene derivatization for covalent immobilization of aptamers, *Carbon* 196 (2022) 264–279.
- [47] M.K. Rabchinskii, et al., A Blueprint for the Synthesis and Characterization of Thiolated Graphene, *Nanomaterials* 12 (1) (2022).
- [48] D. Higgins, et al., The application of graphene and its composites in oxygen reduction electrocatalysis: A perspective and review of recent progress, *Energy Environ. Sci.* 9 (2016) 357–390.
- [49] J. Ederer, et al., Determination of amino groups on functionalized graphene oxide for polyurethane nanomaterials: XPS quantitation vs. functional speciation, *Rsc Adv.* 7 (21) (2017) 12464–12473.
- [50] NIST X-ray photoelectron spectroscopy database..
- [51] W.A. Abdallah, Y. Yang, Raman spectrum of asphaltene, *Energy Fuels* 26 (11) (2012) 6888–6896.
- [52] H.G. Gary, G.E. Handwerk, M.J. Kaiser, 2007, *Petroleum Refining: Technology and Economics*. 5th ed..
- [53] D. Petrauskas, S. Ullah, Manufacture and storage of bitumens. The Shell Bitumen Handbook, Shell International Petroleum Company Ltd, 2015.
- [54] C.L. Chang, H.S. Fogler, Stabilization of asphaltenes in aliphatic solvents using alkylbenzene-derived amphiphiles.1. Effect of the chemical-structure of amphiphiles on asphaltene stabilization, *Langmuir* 10 (6) (1994) 1749–1757.
- [55] G. Gonzalez, A. Middea, Peptization of asphaltene by various oil soluble amphiphiles, *Colloids Surf.* 52 (3–4) (1991) 207–217.
- [56] L. Goual, A. Firoozabadi, Effect of resins and DBSA on asphaltene precipitation from petroleum fluids, *AIChE J.* 50 (2) (2004) 470–479.
- [57] L. Goual, M. Sedghi, Role of ion-pair interactions on asphaltene stabilization by alkylbenzenesulfonic acids, *J. Colloid Interface Sci.* 440 (2015) 23–31.
- [58] S. Noury, L. Krim, Formation of simple nitrogen hydrides NH and NH<sub>2</sub> at cryogenic temperatures through N + NH<sub>3</sub> → NH + NH<sub>2</sub> reaction: dark cloud chemistry of nitrogen, *Phys. Chem. Chem. Phys.* 18 (27) (2016) 18493–18499.
- [59] H.S. Silva, et al., Impact of H-bonds and porphyrins on asphaltene aggregation as revealed by molecular dynamics simulations, *Energy Fuels* 32 (11) (2018) 11153–11164.
- [60] R. Skartlien, S. Simon, J. Sjöblom, A DPD study of asphaltene aggregation: the role of inhibitor and asphaltene structure in diffusion-limited aggregation, *J. Dispers. Sci. Technol.* 38 (3) (2017) 440–450.
- [61] J.D. Liu, et al., Efficient recovery of lithium as Li<sub>2</sub>CO<sub>3</sub> and cobalt as Co<sub>3</sub>O<sub>4</sub> from spent lithium-ion batteries after leaching with p-toluene sulfonic acid, *Hydrometallurgy* 216 (2023) 10.
- [62] B. Li, Characterization of pore structure and surface chemistry of activated carbons – a review, *Fourier Transform - Mater. Anal.* (2012).
- [63] K.C. Chen, et al., Theoretical Studies on the Electronic Structure of Nano-graphenes for Applications in Nonlinear Optics, *Chem. Res. Chin. Univ.* 38 (2) (2022) 579–587.
- [64] J. Ota, et al., Graphene dispersion in hydrocarbon medium and its application in lubricant technology, *RSC Adv.* 5 (66) (2015) 53326–53332.
- [65] S. Weigel, D. Stephan, Relationships between the chemistry and the physical properties of bitumen, *Road. Mater. Pavement Des.* 19 (7) (2018) 1636–1650.
- [66] C.A. Cooke, et al., Polycyclic aromatic compounds in rivers dominated by petrogenic sources after a boreal megafire, *Environ. Sci. Technol.* (2022) 9.
- [67] L. Serrano-Lujan, et al., Environmental impact of the production of graphene oxide and reduced graphene oxide, *Sn Appl. Sci.* 1 (2) (2019) 12.
- [68] U.S. Energy Information Administration - EIA - Independent Statistics and Analysis..
- [69] R. Malhotra, et al., Cytotoxicity survey of commercial graphene materials from worldwide, *Npj 2d Mater. Appl.* 6 (1) (2022) 11.
- [70] A. Kros, R.J.M. Nolte, N. Sommerdijk, Conducting polymers with confined dimensions: Track-etch membranes for amperometric biosensor applications, *Adv. Mater.* 14 (23) (2002) 1779–1782.